J Radioanal Nucl Chem (2016) 307:2035–2046
DOI 10.1007/s10967-015-4404-y

Radiological assessment of pharmaceutical clays

Paulo Sergio Cardoso da Silva[1] · Marcelo Francis Máduar[1] · Marcos Antonio Scapin[1] · Rafael Henrique Lazzari Garcia[1] · João Paulo Machado Martins[1]

Received: 11 June 2015 / Published online: 12 September 2015

Abstract The suitability for pharmaceutical and cosmetic application of fourteen clay samples, eight raw and six commercialized samples, from Minas Gerais and São Paulo states, Brazil, were evaluated and their mineralogy, chemical and radiological composition were determined. Results indicated that the samples are composed mainly of quartz, kaolinite and feldspar, enriched in Al_2O_3 and TiO_2, Cd, Cs, Sb, Se, Th, and U and depleted in SiO_2, MgO, P_2O_5, and Ca. Concentrations found are unlikely to present any harm in topical applications, and all the radiological parameters were below the global average or the established limits.

Keywords Raw clays · Commercialized clays · Therapeutic · Cosmetic · Radionuclides · Dose

Introduction

Clays are natural materials with earthy texture, fine-grained particles of lamellar or fibrous form, consisting mainly of clay minerals and also containing other non-clay minerals, such as quartz, mica, pyrite, hematite, as well as organic matter and other impurities [1, 2]. In the presence of water, clays develop a series of properties such as plasticity, strength, linear shrinkage of drying, thixotropy and viscosity, which explains its wide range of technological applications [3–6].

In cosmetics and pharmaceutical industry clays are used as excipients, lubricants, diluents, binders, desiccants, emulsifiers, thickeners, to mask undesirable flavors, isotonic agent, active substances charger, and delivery [7–11]. These characteristics have contributed to the expansion of the search for clay minerals applications mainly due to the interest in natural products and the environment preservation. In spite of being natural material, clays may not be free of possible adverse health effects when used for therapeutic or cosmetic purposes due to the presence of dangerous minerals to the respiratory system, toxic elements, and the occurrence of radioactive elements [12–14].

The occurrence of toxic elements such as arsenic (As), antimony (Sb), cadmium (Cd), cobalt (Co), copper (Cu), lead (Pb), mercury (Hg), nickel (Ni), selenium (Se), zinc (Zn) as well as radioactive ones, in a wide range of concentrations, depends on the geological origin of the clays. These trace and radioactive elements may be present in the clay structure or adsorbed on its surface; in the latter case mobilization and transference to leaching solutions is considerably easier [15, 16]. Therefore, the use of clays containing these elements in high amounts may present a potential risk for human exposure and increase health risks.

One approach recently used to characterize the impurity content in therapeutic and cosmetic products is the PDE—permitted daily exposure—[17, 18] for drug products, defined as the maximum acceptable exposure to an element that is unlikely to produce any adverse health effect. According to the PDE, the elements As, Cd, and Pb are significantly toxic in oral, parenteral, and inhalation administration routes.

The exposure to naturally occurring radiation accounts for up to 85 % of annual effective dose received by the

✉ Paulo Sergio Cardoso da Silva
pscsivla@ipen.br

[1] Research Reactor Center, Energy and Nuclear Research Institute (Instituto de Pesquisas Energéticas e Nucleares, Av. Prof. Lineu Prestes 2242, Cidade Universitária, São Paulo CEP 05508 000, Brazil

population. This exposure is mainly due to primordial radionuclides which are widely spread and are present in almost all geological materials in the environment. The main sources of natural radiation exposure is therefore due to the presence of the naturally occurring radionuclides belonging to the decay series of ^{235}U, ^{238}U (uranium), ^{232}Th (thorium), and the radionuclide ^{40}K (potassium) [19, 20]. The average crustal abundance of uranium and thorium are 2.8 μg g^{-1} and 10 μg g^{-1} while typical ranges are 1.5–6.5 and 6–20 μg g^{-1}, respectively [21]. Average Th/U ratio in most rocks, in which uranium is not enriched, is 3.5 [22]. These figures can, otherwise, widely vary as a function of the clay origin and clay capacity in adsorbing radioactive elements at its surface.

The objective of this paper is to describe the mineralogical and chemical composition of eight raw and six commercial clays, as well as to determine the radiological parameters arising from its external and internal use, both in cosmetic and pharmaceutical purpose.

Methodology

Sampling location

Raw clay samples (identified as CG samples) were collected in Campos Gerais city in the Southwestern portion of Minas Gerais state, located at about 362 km far from Araxá city, a region known by its high radioactivity background levels. Geologically, the region encompasses the rock assembly positioned between the nappes of Passos and Varginha-Guaxupé in the southern Brasilia Belt. The unit consists of orthogneissic, basic, ultramafic, and associated subordinate metasedimentary rocks, subdivided into two areas: one to the North containing orthogneiss, basic, and ultrabasic rocks and other in the South formed by paragneiss, metapelites, and metamafic rocks of the Jacuí—Bom Jesus da Penha track [23, 24]. The commercial clay samples (identified as SP samples) were obtained in a natural products health store in São Paulo city and the origin of the samples is unknown.

Physical–chemical characterization

The pH was determined by mixing 10 mL of the wet clay sample with 25 mL of KCl 1.0 mol L^{-1}. The solutions were stirred for 5 min, let to stand for 1 h and then the measurement was performed. For moisture, organic matter and loss of ignition the wet samples were treated sequentially at 105, 450 and 1000 °C in an oven furnace and muffle, respectively.

X-ray diffraction

For XRD analysis the samples were oven dried at 105 °C and sieved to a particle size less than 0.065 mm. XRD patterns were obtained in a Rigaku diffractometer, Multiflex model (Rigaku Co, Tokyo, Japan). All samples were analyzed using Cu-Kα radiation at 800 W, in the 2θ range from 3 to 70° with step size of 0.02° and 8 s per step. The results were compared with reference powder diffraction files using the Diffrac EVA version 3.1 software by Bruker.

X-ray fluorescence

The chemical characterization, performed in the oven dried samples at 105 °C and sieved to a grain size less than 0.065 mm, was carried out using a WDXRF spectrometer Rigaku Co., model RIX 3000 (Rigaku Co, Tokyo, Japan) with X-ray tube with Rh anode, a 75 μm Be window, and a 60 kV maximum acceleration voltage, scintillation detector NaI(Tl) and flow-proportional counter. The pellets of sample were made by mixing, in a Mixer/Miller, 1.8 g or sample with 0.2 g of powder wax (analytical grade, Hoechst), to make homogeneous. This mixture was finally pressed in order to form the pellets. The Fundamental Parameters method was applied for correction of the absorption/excitation effects. The methodology was evaluated, using standard reference material SRM 2709—San Joaquin Soil and SRM 2711—Montana Soil, from NIST (National Institute of Standards & Technology).

Neutron activation analysis

The elements As, bromine (Br), Co, chromium (Cr), cesium (Cs), iron (Fe), hafnium (Hf), K, magnesium (Mg), manganese (Mn), sodium (Na), rubidium (Rb), Sb, scandium (Sc), Se, tantalum (Ta), titanium (Ti), vanadium (V), Zn, zirconium (Zr) and rare earth elements: cerium (Ce), europium (Eu), lanthanum (La), lutetium (Lu), neodymium (Nd), samarium (Sm), terbium (Tb), and ytterbium (Yb), were determined by instrumental neutron activation analysis (INAA) in short and long irradiations periods (15 s and 8 h, respectively). For multi-elemental analysis, approximately 60 mg of sample and 100 mg of reference material (estuarine sediment, NIST SRM 1646a and Syenite, Table Mountain, STM-2 from USGS) were weighed and sealed in pre-cleaned double polyethylene bags for short and long irradiations. Synthetic standards were also prepared from standard solutions (SPEX Certiprep Inc., USA). Samples and reference materials were irradiated in a thermal neutron flux of 1012 cm^{-2} s^{-1} at the IEA-R1 nuclear research reactor at IPEN (Instituto de Pesquisas Energéticas e Nucleares). The counting time was 3 min for

short and 2 h long irradiation, after the necessary decay period for each target nuclide using an EG&G Ortec Ge high pure Gamma Spectrometer detector (AMETEK Inc., USA) and associated electronics, with a resolution of 0.88 and 1.90 keV for ^{57}Co (122 keV) and ^{60}Co (1332 keV), respectively [25]. Analysis of the data was carried out by using an in-house gamma ray software, VISPECT program, to identify the gamma-ray peaks.

Graphite furnace atomic absorption spectrometry (GFAAS)

For the Cd and Pb determination by GFAAS, approximately 0.30 g of dried samples were dissolved in a microwave closed system with concentrated nitric, hydrochloric, hydrofluoric acids and hydrogen peroxide 30 % (Merck, Darmstadt, Germany). The digested samples were allowed to cool at room temperature and diluted with high-purity Milli-Q water 18.2 MΩ cm^{-1} at 25 °C (Millipore Corporation, USA).

Measurements were performed by using a Perkin Elmer AAnalyst 800 graphite furnace atomic absorption spectrometer (Perkin Elmer, Vernon Hills, Illinois, USA). Calibration curve coefficients were obtained by a linear regression fit with least-squares method performed by the spectrometer software. Matrix modifier of $NH_4H_2PO_4$ 0.5 % (m/v) and $Mg(NO_3)_2$ 0.03 % (m/v) were used to avoid chemical interferences. The blanks were prepared and analyzed by using the same procedure applied to the samples. Analyses were carried out in duplicate with differences between the measurements up to 10 %. The detection limits for Cd and Pb were determined using the IUPAC criterion, and the values obtained were 0.016 and 0.85 mg kg^{-1}, respectively [26].

Gamma-ray spectrometry

Activity concentrations of ^{226}Ra, ^{228}Ra (radium), ^{210}Pb (lead) and ^{40}K were determined by gamma-ray spectrometry employing a Canberra GX2520 high purity germanium detector (HPGe) with nominal efficiency of 25 % at 1332 keV gamma energy and a beryllium window for extended low energy detection. The detection system was calibrated with soil, rock and water matrices spiked with radionuclides certified by Amersham. Samples were placed in 100 cm^3 polyethylene flasks, sealed and set apart for about 4 weeks prior to the measurements to ensure reaching of radioactive equilibrium between ^{226}Ra and its short-living decay products. Activities of ^{226}Ra were determined by taking the mean activity of three separate photopeaks from its decay products: ^{214}Pb at 295 and 352 keV, and ^{214}Bi (bismuth) at 609 keV. For ^{228}Ra content of the samples, 911 and 968 keV photopeaks from ^{228}Ac (actinium) were employed. Concentration of ^{210}Pb was determined by measuring the activity of its low energy gamma ray peak (46.5 keV). The corrections for self-attenuation were performed by placing a ^{210}Pb point source above each sample and counting to estimate individual attenuation factors, according to the procedure described in Cutshall et al. [27].

Results

Physical–chemical clay properties

Figure 1 summarizes the pH, moisture, organic matter and loss on ignition (LOI) for the 14 analyzed clay samples. Among the raw clays, moisture was higher in samples CG1 and CG5 and among the commercialized clays, in samples SP9 and SP12. Organic matter was generally lower in commercialized clays rather than the raw ones while for LOI the contrary was observed. The value of pH varied from 3.6 to 7.8 for all samples and as a rule, all the analyzed clays produced acidic solutions.

Clays mineralogy

The main minerals obtained by XRD in the samples are summarized in Table 1. The results indicated that quartz and kaolinite are present in all samples, and, with respect to peak intensities, were major minerals for the majority of the samples. Mica minerals were present in nine samples, being five of them raw clays, and four of them, commercial clays. Feldspar minerals were present in three raw clays and three commercial samples, and minerals from the magnetite group were found in six raw clays and one commercial sample.

Chemical characterization

For chemical characterization XRF, INAA and GFAAS were applied and the results are shown in Tables 2 and 3. Table 2 presents the results for major and trace elements while in Table 3 the rare earth concentrations are shown. For comparison purpose the upper continental crust (UCC) values are also showed in these tables [28]. These results showed that SiO_2 and Al_2O_3 were the main constituents of all samples in connection with the amount of quartz and kaolinite present. The mica amount contributes both to K and Al content. In the same way, the iron content must be related to the presence of Fe-bearing minerals, probably magnetite and hematite. All the samples are enriched in Al_2O_3 and TiO_2 and depleted in SiO_2, MgO, P_2O_5 and Ca, related to UCC.

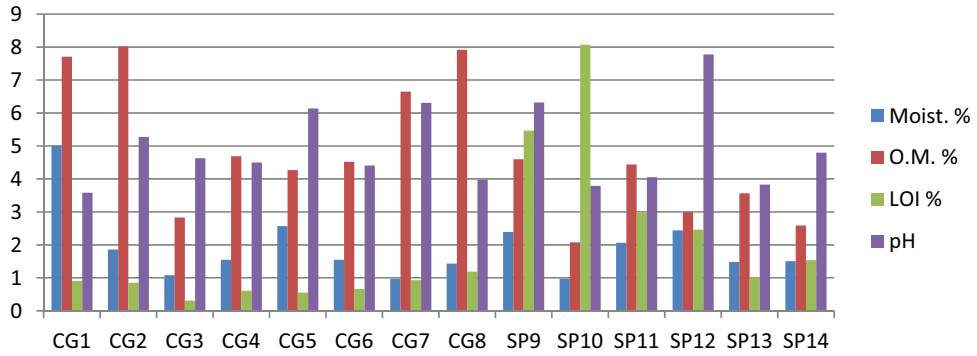

Fig. 1 Percentage of moisture, organic matter, loss on ignition and pH values for the raw and commercialized clays

Table 1 Mineral groups determined in the raw (CG) and commercialized (SP) clay samples by XRD

Mineral	CG1	CG2	CG3	CG4	CG5	CG6	CG7	CG8	SP9	SP10	SP11	SP12	SP13	SP14
Quartz	x	x	x	x	x	x	x	x	x	x	x	x	x	x
Kaolinite	x	x	x	x	x	x	x	x	x	x	x	x	x	x
Gibbsite					x	x								
Mica	x	x	x	x			x		x			x	x	x
Palygorskite												x		
Magnetite	x	x			x	x	x	x			x			
Microcline feldspar			x	x		x			x					
Orthoclase feldspar												x		x

The concentrations of trace elements vary across a wide range (Table 2). The elements Cd, Cs, Sb, Se, Th and U show a tendency of being enriched in the commercialized samples that also tend to be more enriched when compared to the UCC values. Since commercialized clays are composed of only the silt and clay fraction which are known to possess high ion exchange capacity commercial clay will concentrate higher amount of trace elements [29, 30]. Zinc and Hf are enriched over UCC in almost all the samples and Ba and Br are the only two elements that tend to be higher than UCC in the raw samples.

The Th/U ratio calculated for the samples presented a low value in the samples CG1, CG2 and SP9. For all other samples this ratio varied from 3.9 to 5.6, close to the theoretical value of 3.5 to 4.0 [31]. Low values of the Th/U ratios were related to the redox environment in the clay deposit. Under reduction conditions U mainly exist as U^{4+}, much less mobile then its oxidized form U^{6+} [32].

Except for the samples CG5, CG7, CG8, SP9 and SP11 all the other samples were enriched in rare earth elements (Table 3) related to UCC while only the samples CG3, CG8 and SP10 presented the light rare earth elements (LREE) enriched over the heavy rare earth elements (HREE).

The activity concentrations of the radionuclides ^{226}Ra, ^{210}Pb, ^{228}Ra and ^{40}K are shown in Table 4 together with the activity concentrations of ^{238}U and ^{232}Th. Compared to the median soil values, the commercialized samples showed higher activity concentrations than raw samples [33].

Discussion

The pH of the presented samples were generally lower than that reported by Lopes-Galindo et al. [14] and Silva et al. [34] for clays used for therapeutic and cosmetic purposes.

Loss on ignition at 1000 °C was mainly related to carbonate content in the sample and certain volatile non-carbon components such as gypsum, sulphide minerals, and dehydration of metallic oxyhydroxides [35]. It was observed that the raw clay samples had a LOI that was considerably lower than the commercialized samples. Although, organic matter was higher in raw samples.

The sample distributions according to their similarities were obtained by the application of cluster analysis are shown in Fig. 2. The origin of the clays clearly separate in two groups, being group one composed of the raw samples from Campos Gerais and group two composed of the commercialized samples from São Paulo. Only raw CG6 sample displayed heightened similarity to the commercialized samples due to the trace and rare earth element

Table 2 Major elements and trace elements content in raw (CG) and commercialized (SP) clays

	CG1	±	CG2	±	CG3	±	VG4	±	CG5	±	CG6	±	CG7	±	CG8
%															
SiO_2	48	2	49	2	62	2	54	2	60	2	56	2	49	2	46
Al_2O_3	24	2	27	2	17	2	26	2	24	2	28	2	27	2	31
TiO_2	1.6	0.4	1.1	0.2	0.8	0.2	1.7	0.4	0.9	0.2	0.7	0.2	1.2	0.2	1.0
MgO	1.1	0.2	1.1	0.2	0.2	0.1	1.9	0.2	0.3	0.2	0.8	0.2	0.4	0.2	0.4
P_2O_5	0.08	0.02	0.07	0.02	0.06	0.02	0.04	0.02	0.05	0.02	0.06	0.02	0.05	0.02	0.04
MnO	0.03	0.02	0.09	0.02	< 0.01		0.05	0.02	0.03	0.02	0.03	0.01	0.10	0.05	0.04
NiO	0.02	0.01	0.02	0.01	< 0.01		0.02	0.01	0.02	0.02	0.02	0.01	0.02	0.01	0.02
CuO	0.02	0.01	0.02	0.01	< 0.01		0.02	0.01	< 0.01		< 0.01		0.02	0.01	< 0.01
SO_3	<0.01		0.04	0.02	0.03	0.02	0.03	0.01	0.03	0.02	< 0.01		0.04	0.01	0.04
Fe	4.4	0.1	5.1	0.1	0.79	0.02	2.28	0.06	2.62	0.08	3.0	0.1	4.1	0.1	3.6
K	0.9	0.2	1.1	0.4	2	1	1.5	1	0.6	0.2	2.1	0.4	1.0	0.4	1.4
Ca	0.4	0.2	0.4	0.2	0.16	0.08	0. 5	0.1	0.15	0.1	0.7	0.2	0.3	0.1	0.20
µg/g															
As	ND		ND		ND		ND		2.4	0.2	0.6	0.4	3.1	0.2	2.4
Ba	160	60	355	80	1894	230	746	120	167	60	737	182	298	90	353
Br	6.0	0.8	1.3	0.4	4.7	0.4	2.6	0.6	2.7	0.1	1.3	0.4	1.56	0.08	1.28
Co	7.9	0.2	48	1	1.7	0.1	14.1	0.4	3.5	0.8	14	2	6	1	4
Cr	144	10	100	6	18	2	85	6	40	2	52	4	46	2	45
Cs	2.3	0.2	3.3	0.4	1.7	0.2	3.7	0.2	0.9	0.4	2.3	0.4	0.9	0.2	0.78
Hf	6.0	0.4	8.1	0.4	15.0	0.8	9.7	0.4	7.2	0.6	15	1	7.0	0.2	ND
Na	523	62	99	24	1865	150	698	50	139	10	5145	300	180	10	219
Pb	24.27	0.04	17.5	0.1	36.0	0.2	21.2	0.4	6.7	0.2	14.2	0.2	8.20	0.04	11.54
Rb	31	6	40	6	93	8	135	8	7	4	57	8	11	3	18
Sb	0.2	0.1	0.4	0.1	ND		0.12	0.04	0.23	0.04	0.09	0.06	0.25	0.06	0.24
Sc	28.6	0.4	14.5	0.2	6.4	0.1	16.3	0.2	6.4	0.1	10.2	0.2	8.7	0.1	9.6
Se	ND		0.4	0.2	0.3	0.2	0.2	0.1	ND		ND		0.3	0.1	ND
Th	7.9	0.2	7.2	0.2	ND		11.4	0.2	3.4	0.2	7.6	0.2	3.9	0.2	3.7
U	3.1	0.4	4	1	1.7	0.2	2.0	0.1	0.8	0.1	1.9	0.4	1.00	0.2	0.9
Zn	546	22	476	20	294	12	371	14	197	14	301	20	246	18	37
Th/U	2.6		1.9				5.6		4.4		4.0		3.9		4.1
ng/g															
Cd	22. 2	0.6	53	10	20	1	33	4	6	4	13.2	0.2	12	1	10

	SP9	±	SP10	±	SP11	±	SP12	±	SP13	±	SP14	±	UCC*
%													
SiO_2	50	2	57	2	53	2	50	2	56	2	66	2	66.62
Al_2O_3	36	2	29	2	27	2	14	2	21	2	18	2	15.4
TiO_2	0.13	0.05	1.6	0.4	1.8	0.4	0.5	0.2	0.8	0.2	0.4	0.2	0.64
MgO	0.16	0.05	0.17	0.05	0.4	0.2	1.1	0.2	0.5	0.2	1.2	0.2	2.48
P_2O_5	< 0.01		0.03	0.01	0.11	0.05	0.13	0.05	0.04	0.01	0.02	0.01	0.15
MnO	0.02	0.01	< 0.01		0.02	0.01	0.07	0.01	< 0.01		0.05	0.01	0.1
NiO	0.02	0.01	0.02	0.01	0.02	0.01	0.02	0.01	0.02	0.01	< 0.01		
CuO	< 0.01		0.02	0.01	< 0.01		< 0.01		< 0.01		< 0.01		
SO_3	0.05	0.01	0.08	0.02	0.16	0.05	0.17	0.05	0.03	0.01	0.02	0.01	
Fe	0.67	0.02	0.52	0.02	4.15	0.08	2.51	0.03	1.41	0.02	2.84	0.03	3.53
K	1.0	0.1	0.4	0.2	2.1	0.6	2.7	0.6	1.9	0.4	4.1	0.8	2.3
Ca	0.8	0.2	1.2	0.4	1.2	0.4	1.3	0.4	0.6	0.2	0.5	0.2	2.56
µg/g													

Table 2 continued

	SP9	±	SP10	±	SP11	±	SP12	±	SP13	±	SP14	±	UCC*
As	ND		2.5	0.6	21	2	4.2	0.8	2.4	0.8	10	1	4.8
Ba	354	46	125	40	185	25	381	60	95	20	736	98	624
Br	0.8	0.2	0.8	0.6	5.4	0.4	ND		0.5	0.6	0.6	0.6	1.6
Co	5.1	0.2	17.4	0.6	4.9	0.2	6.5	0.2	2.5	0.2	9.6	0.4	17.3
Cr	4.4	0.8	57	4	50	4	37	2	33	2	45	2	92
Cs	4.2	0.8	11	2	9	2	8	1	8	1	9	2	4.9
Hf	2.10	0.08	14.9	0.4	11.0	0.4	6.2	0.2	11.8	0.4	9.6	0.2	5.3
Na	4513	200	557	30	346	20	5594	260	628	42	6689	300	24260
Pb	16.6	0.04	30	0.2	121	6	19.7	0.8	29	1	20.8	0. 4	17
Rb	98	10	44	6	51	10	164	18	86	10	179	20	84
Sb	0.4	0.2	1.9	0.6	1.9	0.6	1.6	0.4	2.0	0.6	1.9	0.4	0.4
Sc	1.60	0.04	12.2	0.1	13.8	0.2	9.5	0.1	11.7	0.1	10.6	0.1	14
Se	0.4	0.2	1.9	0.6	1.1	0.6	1.4	0.5	ND		1.6	0.6	0.09
Th	4.3	0.6	21	2	15	2	16	2	18	2	17	2	10.5
U	5.2	0.6	4.7	0.8	2.9	0.6	5.3	0.8	3.6	0.8	3.1	0.2	2.7
Zn	116	14	314	36	147	18	118	14	113	14	159	18	67
Th/U	0.8		4.6		5.0		3.1		4.8		5.4		3.9
ng/g													
Cd	71.8	0.4	71	1	16	4	105	1	51	2	68	10	90

(±) Expanded uncertainties ($K = 2$)

ND not determined, *UCC* upper continental crust [26]

Table 3 Rare earth element concentrations, in μg/g, determined by INAA in raw (CG) and commercialized (SP) clay samples

	CG1	CG2	CG3	VG4	CG5	CG6	CG7	CG8
La	43.3 ± 0.8	153 ± 2	105 ± 2	49.1 ± 0.8	2.87 ± 0.04	46.3 ± 0.6	4.64 ± 0.08	5.9 ± 0.1
Ce	71 ± 2	80 ± 4	165 ± 6	92 ± 4	53 ± 4	92 ± 4	33 ± 2	26 ± 1
Nd	33 ± 4	120 ± 20	85 ± 10	48 ± 8	ND	23 ± 4	3 ± 1	7 ± 1
Sm	9.2 ± 0.2	33.8 ± 0.6	23.1 ± 0.2	11.3 ± 0.2	0.53 ± 0.01	9.4 ± 0.2	0.75 ± 0.02	0.93 ± 0.02
Eu	1.85 ± 0.08	5.7 ± 0.2	ND	2.10 ± 0.06	0.09 ± 0.04	1.34 ± 0.08	0.16 ± 0.02	0.19 ± 0.02
Tb	1.0 ± 0.2	3.1 ± 0.4	2.4 ± 0.2	1.21 ± 0.08	ND	1.1 ± 0.2	ND	0.11 ± 0.08
Yb	3.3 ± 0.4	6.4 ± 0.6	4.5 ± 0.4	3.0 ± 0.2	0.3 ± 0.2	2.4 ± 0.4	0.3 ± 0.1	0.38 ± 0.04
Lu	0.58 ± 0.04	1.17 ± 0.06	0.76 ± 0.04	0.56 ± 0.02	0.08 ± 0.02	0.42 ± 0.04	0.08 ± 0.02	0.10 ± 0.02
LREE	158.6	392.9	377.8	202.2	56.5	172.1	42.2	40.5
HREE	4.9	10.7	7.7	4.7	0.4	3.9	0.4	0.6

	SP9	SP10	SP11	SP12	SP13	SP14	UCC
La	12.4 ± 0.4	49 ± 2	21.8 ± 0.8	37.6 ± 0.7	68 ± 1	42.3 ± 0.8	31
Ce	20 ± 1	89 ± 6	46 ± 4	72 ± 3	161 ± 6	81 ± 3	63
Nd	14 ± 6	45 ± 7	17 ± 4	36 ± 5	77 ± 10	44 ± 7	27
Sm	2.4 ± 0.2	7.1 ± 0.6	3.8 ± 0.4	6.4 ± 0.3	12.4 ± 0.5	8.3 ± 0.3	4.3
Eu	1.03 ± 0.06	1.31 ± 0.08	0.58 ± 0.04	1.16 ± 0.04	2.54 ± 0.07	1.43 ± 0.05	1
Tb	0.25 ± 0.08	1.3 ± 0.2	0.4 ± 0.2	1.1 ± 0.1	2.1 ± 0.2	1.1 ± 0.1	0.7
Yb	1.0 ± 0.2	1.9 ± 0.4	2.2 ± 0.4	2.7 ± 0.2	5.1 ± 0.4	3.5 ± 0.3	2
Lu	0.20 ± 0.02	0.59 ± 0.04	0.46 ± 0.04	0.47 ± 0.02	0.91 ± 0.04	0.61 ± 0.03	0.31
LREE	49.8	191.4	89.2	152.9	320.9	176.4	126.3
HREE	1.5	3.8	3.0	4.3	8.1	5.2	3.0

(±) Expanded uncertainties ($K = 2$)

ND not determined, *UCC* upper continental crust [26]

Table 4 Activity concentrations, in Bq/kg, for the raw (CG) and commercialized (SP) clays

	CG1	CG2	CG3	VG4	CG5	CG6	CG7	CG8	SP9	SP10	SP11	SP12	SP13	SP14	Soil[a]
U-238	38 ± 4	46 ± 6	21 ± 4	25 ± 2	10 ± 2	24 ± 4	12 ± 2	11 ± 2	65 ± 8	58 ± 8	36 ± 4	67 ± 7	45 ± 5	39 ± 4	35
Ra-226	37 ± 2	25 ± 1	30 ± 1	33 ± 1	10.1 ± 0.8	25 ± 1	18 ± 1	19 ± 1	95 ± 4	82 ± 4	40 ± 2	67 ± 2	57 ± 2	42 ± 2	35
Pb-210	44 ± 12	26 ± 5	42 ± 10	±7	20 ± 4	31 ± 10	20 ± 5	23 ± 5	118 ± 18	99 ± 20	42 ± 10	94 ± 20	±10	49 ± 9	
Th-232	32 ± 1	29.1 ± 0.8	ND	46 ± 1	14.0 ± 0.6	31 ± 1	15.9 ± 0.8	14.8 ± 0.6	18 ± 2	86.4 ± 10	59.0 ± 7	66.2 ± 8	71 ± 8	68 ± 8	30
Ra-228	31 ± 3	28 ± 2	40.3 ± 3	52 ± 3	15 ± 2	27 ± 1	29.6 ± 2	25 ± 2	18 ± 2	91 ± 4	61 ± 4	65 ± 2	70 ± 2	71 ± 4	30
K-40	150 ± 10	211 ± 12	736 ± 70	738 ± 70	118 ± 16	418 ± 42	196 ± 20	293 ± 30	306 ± 40	183 ± 30	107 ± 11	±80	437 ± 40	1213 ± 100	400

(±) Expanded uncertainties ($K = 2$);

ND not determined

[a] Average soil concentration [33]

content. Besides the provenance, other features that also contributed to these group formations were the granulometric fraction and accessory minerals presented in the samples reflected by the elementary concentration.

Figure 3 shows the element pattern of similarities obtained by cluster analysis. The results show an association among the radionuclides of the uranium and thorium series with the content of SiO_2 and Al_2O_3, therefore, indicating that the kaolinite must be the main mineral driving these element concentrations.

Considering the potentially toxic elements, only the sample SP11 presented an As concentration above the PDE limit (15 μg day^{-1}) and this concentration could be a threat for health. All the samples had a higher PDE value for Pb, 5 ug/day, which makes both raw and commercialized clays inappropriate for ingestion applications. On the other hand topic applications could not be a risk due to the very low dermal absorption for lead [36]. All samples were below the PDE value for Cd, which is 5 ug/day.

Radiological parameters were calculated for the use of the analyzed clays for pharmaceutical and cosmetic purposes and the results are shown in Table 5. With regard to biological effects, the radiological and clinical effects are directly related to the absorbed dose rate.

The world dose rate average is 84 nGy/h and this value was exceeded in the commercialized samples SP10, SP12, SP13 and SP14.

The annual effective dose equivalent (AEDE) takes into consideration the adsorbed dose rate and also the time spent in contact with the radioactive source. The AEDE resulting from the exposure to the analyzed clays varied from 4.9 to 29.2 μSv/y, these values were much lower than the global indoor AEDE average: 450 μSv/y [37].

Excess life time cancer risk (ELCR) is the risk of fatal cancer occurring during a life time (DL) of 70 years that also takes into consideration the annual effective dose equivalent (AEDE) and a risk factor (RF in Sv^{-1}) established as 0.05 by the ICRP 60 for stochastic effects for the public [38].

The calculated ELCR varied from 1.7×10^{-5} to 10.2×10^{-5} in the samples which was also lower than the average world of 29×10^{-5} [33].

Another radiological parameter, annual genetically significant dose equivalent (AGDE) is a measure of the genetic significance of the dose equivalent received by the population's reproductive organs per year [39].

The International Commission on Radiological Protection [40] recommends a dose increment less than 1 mSv/y for the general public. All the clay samples showed values lower than this limit.

As clays are generally used as excipient in medicine formulations, its ingestion is also of radiological concern. Once in the body radionuclides are typically accumulated

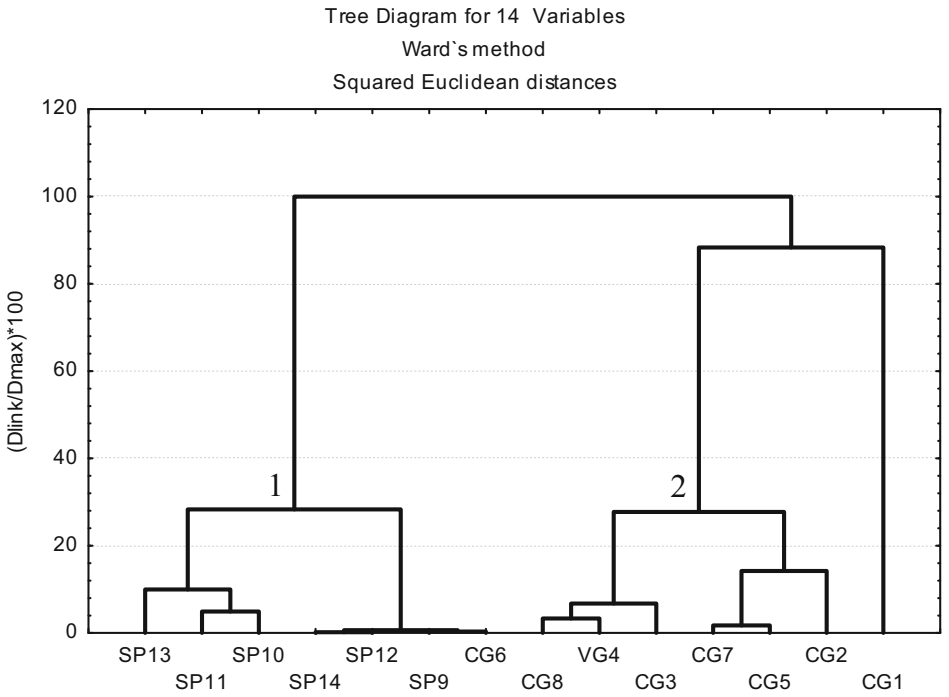

Fig. 2 Dendrogram of similarity pattern of the samples obtained by Cluster Analysis

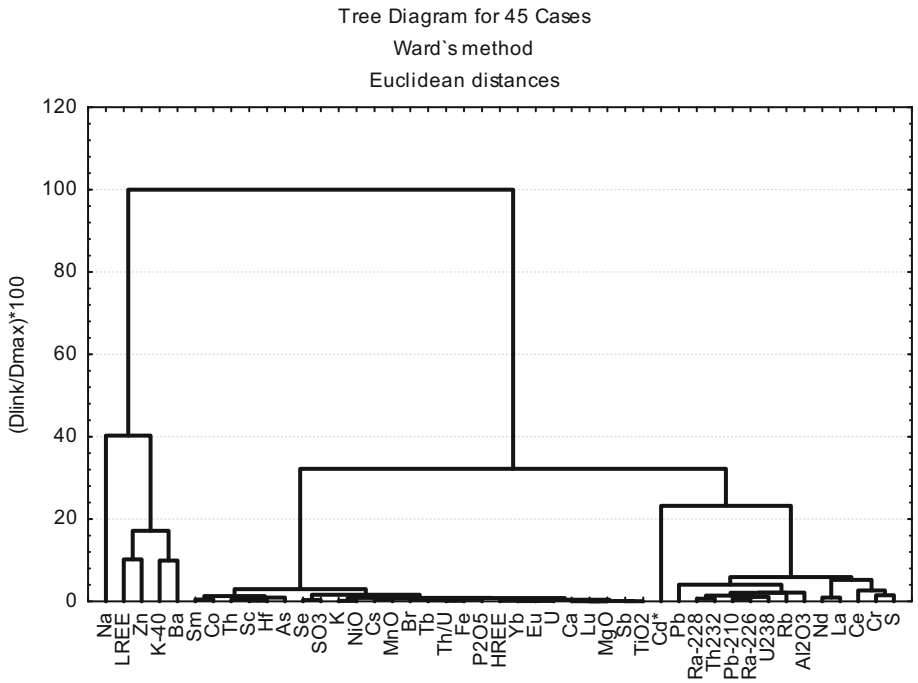

Fig. 3 Dendrogram of similarity pattern of the elements obtained by Cluster Analysis

in the skeleton, liver, kidney and soft tissues, although not being entirely retained in the organism. The International Commission on Radiological Protection [41] provides recommendations and guidelines on all aspects of protection against ionizing radiation and it has presented fractional absorption which describes the proportion that is absorbed from radionuclides ingestion. Dose coefficients allow the determination of effective dose associated with radiation exposure in assessing the health risk.

The annual effective dose (E_{ing}) due to clay ingestion was calculated as follows:

$$E(\mu\text{Sv/y}) = \sum Ai(\text{Bq/kg}) \times \text{DC(Sv/Bq)} \times I(\text{kg/y}) \times 10^6 \quad (1)$$

Table 5 Radiological parameters: dose rate (DR), annual effective dose equivalent (AEDE), excess life time cancer risk (ELCR), annual genetically significant dose equivalent (AGDE), annual effective dose (E_{ING}) for ingestion, determined for the raw (CG) and commercialized (SP) clays

	CG1	CG2	CG3	VG4	CG5	CG6	CG7	CG8
DR (nGy/h)	43.4 ± 1	39.1 ± 1	43.7 ± 2	75.8 ± 2	18.6 ± 1	49.0 ± 2	26.7 ± 1	30.3 ± 1
AEDE (mSv/y)	11.1 ± 0.3	10.0 ± 0.3	11.2 ± 0.5	19.4 ± 0.5	4.8 ± 0.2	12.5 ± 0.4	6.8 ± 0.2	7.7 ± 0.3
ELCR × 10^{-5}	3.9 ± 0.1	3.0 ± 0.1	3.9 ± 0.2	6.8 ± 0.2	1.7 ± 0.1	4.0 ± 0.1	2.4 ± 0.1	2.7 ± 0.1
AGDE (mSv/y)	294.6 ± 8	265.7 ± 7	323.2 ± 13	526.0 ± 15	126.6 ± 5	338.7 ± 11	184.5 ± 7	212.3 ± 8
E_{ING} (μSv/y)	26 ± 2	19 ± 2	25 ± 2	34 ± 2	11.3 ± 1	21 ± 2	16.1 ± 2	15.9 ± 2
	SP9	SP10	SP11	SP12	SP13	SP14		
DR (nGy/h)	65.3 ± 2	100.7 ± 5	61.1 ± 3	107.5 ± 5	90.2 ± 4	114.2 ± 6		
AEDE (mSv/y)	16.7 ± 0.6	25.7 ± 1.2	15.6 ± 0.9	27.5 ± 1.3	23.0 ± 1.1	29.2 ± 1.4		
ELCR × 10^{-5}	5.8 ± 0.2	9.0 ± 0.4	5.5 ± 0.3	9.6 ± 0.4	8.1 ± 0.4	10.2 ± 0.5		
AGDE (mSv/y)	462.1 ± 16	673.4 ± 32	404.5 ± 22	742.3 ± 34	610.3 ± 28	794.2 ± 38		
E_{ING} (μSv/y)	46.4 ± 3	63.5 ± 4	35.0 ± 3	54.4 ± 4	45.3 ± 3	42.5 ± 3		

(±) Expanded uncertainties ($K = 2$)

Table 6 Input parameters for application of VARSKIN 3 code

Parameter	Value
Source geometry	2-D disk
Skin density thickness	7 mg cm^{-2}
Air gap thickness	0 mm
Protective clothing thickness	0 mm
Protective clothing density	0 g cm^{-3}
Source diameter	According to the source area
Source area	2000 and 20,000 cm^2
Irradiation time	100 h
Irradiation area	2000 and 20,000 cm^2

where *Ai* is the activity concentration of the nuclide *i*, DC is the dose coefficient conversion factor and I is the yearly total amount of ingested clay.

The annual effective dose obtained varied from 11 to 63.5 μSv, lower than 0.1 %, of the permitted dose increment of 1 mSv/y.

A more realistic approach to estimate the gamma radiation dose received by the use of cosmetic products is to simulate its application in parts or in the entire body. So that the radiological implications of using the raw and commercialized clays in topical applications were also evaluated by performing a modeling in which a deterministic computer code was used to calculate the absorbed dose to the skin, from the activity concentrations and exposure geometry, VARSKIN 3 [42]. To this calculation, the clay radionuclide concentrations of ^{226}Ra, ^{228}Ra, ^{210}Pb, ^{40}K, ^{232}Th and ^{238}U determined in the samples were applied to the code. Clay application is modeled as a 2-dimensional source disk, directly placed on the skin. Input parameters for VARSKIN 3 are shown in Table 6.

For the assessment, two scenarios were considered, by applying the respective input set to each one:

- Scenario 1: The parameters simulate 1 kg of the clay distributed in a 2-D disk with an area of 20,000 cm^2, corresponding to the total body surface area of a male adult [46]. This is the situation when the clay is applied over large portions of the body.
- Scenario 2: The parameters simulate 1 kg of the clay distributed in a 2-D disk, with area of 2,000 cm^2, which is 10 % of the total body surface area of a male adult, simulating the situation when the clay is applied over one of the legs of the patient.

In both scenarios, a total time of 100 h of clay application was assumed.

According to the procedure described in the ICRP Publication 103 [43], the equivalent dose H_T was assessed by

$$H_T = \sum_R D_{T,R} \times w_R \quad (2)$$

where, H_T is the equivalent dose absorbed by tissue T, DT, R is the absorbed dose in tissue T by radiation type R and w_R is the radiation weighting factor, equal to 1 for both beta and gamma radiation. As the application involves exclusively the topic application on the skin, the effective dose E was assessed as

$$E = \sum_T w_T \times H_T \quad (3)$$

Table 7 Effective dose in the skin (EDS), for a hypothetical treatment with application of clays on the skin, determined for the raw and commercialized clays

	CG1	CG2	CG3	VG4	CG5	CG6	CG7	CG8	SP9	SP10	SP11	SP12	SP13	SP14
EDS_1 (μSv/y)	1.40 ± 0.03	1.90 ± 0.05	6.6 ± 0.3	6.7 ± 0.2	1.1 ± 0.6	3.8 ± 0.2	1.80 ± 0.07	2.60 ± 0.09	2.80 ± 0.09	1.70 ± 0.08	1.00 ± 0.05	7.5 ± 0.3	3.9 ± 0.2	10.9 ± 0.7
EDS_2 (μSv/y)	11.9 ± 0.3	16.7 ± 0.4	58 ± 3	58 ± 2	9.4 ± 0.5	33 ± 1	15.5 ± 0.6	23.2 ± 0.8	24.3 ± 0.7	14.6 ± 0.7	8.5 ± 0.4	66 ± 3	35 ± 2	96 ± 5

EDS_1 and EDS_2 refer respectively to the scenarios of 100 h application on the whole body and on a single leg

(±) Expanded uncertainties ($K = 2$)

where, w_T is the tissue weighting factor, equal to 0.01 for the skin.

The effective doses calculated for the application of each clay are shown in Table 7. The maximum effective doses due to both beta and gamma radiation on the skin, during the treatment time span of 100 h, was 11 μSv, for whole body application, and 96 μSv for application over 10 % of the body's surface.

The final results for the effective dose to the member of the public, in both scenarios, were below the reference level of 1 mSv per year, for the members of the public. Therefore, the radiation dose to the public arising from the dermal application of the clays for cosmetic purpose can be considered negligible.

Conclusions

Eight raw clays from Campos Gerais, Minas Gerais state and six commercialized clays from São Paulo state were analyzed to determine their suitability for pharmaceutical and cosmetic application. Mineralogically, XRD results showed that the samples are composed mainly of quartz and kaolinite. Feldspar, mica and Fe-bearing minerals were also present. Chemically, the main constituents of all the samples were SiO_2 and Al_2O_3. Related to UCC, the analyzed clays were enriched in Al_2O_3 and TiO_2, and depleted in SiO_2, MgO, P_2O_5 and Ca.

Both clays from Campos Gerais and São Paulo showed trace element concentrations in a wide range of elements Cd, Cs, Sb, Se, Th, and U. These trace elements were enriched in the commercialized samples compared to the raw clays.

Only the Pb concentrations for all samples were well above the PDE level for ingestion, while, As had only one sample, SP 11, above the PDE ingestion limit, and all the Cd samples were well below the PDE limit. The concentrations level found for all the analyzed clays were unlikely to present any harm in topical applications due to the low skin absorption of As, Cd and Pb.

The activity concentrations of the radionuclides ^{238}U, ^{232}Th, ^{226}Ra, ^{228}Ra, and ^{210}Pb are lower in the average soils than the raw clays and higher in the commercialized ones. All the radiological parameters were below the global average or the established limits indicating that from the radiological risk point of view all the samples are safe for dermatological and ingestion use.

References

1. Vaccari A (1999) Clays and catalysis: a promising future. Appl Clay Sci 14(4):61–198

2. Harvey CC, Lagaly G (2006) Conventional applications. In: Bergaya F, Theng BKG, Lagaly G (eds) Developments in clay science, vol 1. Elsevier, Amsterdam, pp 501–540
3. Gatica JM, Vidal H (2010) Non-cordierite clay-based structured materials for environmental applications. J Hazard Mater 181(1–3):9–18
4. Rodrigues LAS, Figueiras A, Veiga F, Freitas RM, Nunes LCC, Silva Filho EC, Leite CMS (2013) The systems containing clays and clay minerals from modified drug release: a review. Colloids Surf B 103(1):642–651
5. Dondi M, Raimondo M, Zanelli C (2014) Clays and bodies for ceramic tiles: reappraisal and technological classification. Appl Clay Sci 96:91–109
6. Maisanaba S, Gutiérrez-Praena D, Puerto M, Moyano R, Blanco A, Jordá M, Cameán AM, Aucejo S, Jos Á (2014) Effects of the subchronic exposure to an organo modified clay mineral for food packaging applications on Wistar rats. Appl Clay Sci 95:37–40
7. Veniale F, Barberis V, Carcangiu V, Morandi N, Setti M, Tamanini V, Tessier V (2004) Formulation of muds for pelotherapy: effects of "maturation" by different mineral waters. Appl Clay Sci 25:135–148
8. Choy J, Choi S, Oh J, Park T (2007) Clay minerals and layered double hydroxides for novel biological applications. Appl Clay Sci 36(1–3):122–132
9. Carretero MI, Pozo M (2009) Clay and non-clay minerals in the pharmaceutical industry: part I. Excipients and medical applications. Appl Clay Sci 46:73–80
10. Carretero MI, Pozo M, Martín-Rubí JA, Pozo E, Maraver F (2010) Mobility of elements in interaction between artificial sweat and peloids used in Spanish spas. Appl Clay Sci 48:506–515
11. Ngun BK, Mohamad H, Sulaiman SK, Okada K, Ahmad ZA (2001) Some ceramic properties of clays from central Cambodia. Appl Clay Sci 53(1):33–41
12. Vreca P, Dolonec T (2005) Geochemical estimation of copper contamination in the healing mud from Makirina Bay, central Adriatic. Environ Int 31:53–61
13. Cara S, Carcangiu G, Padalino G, Palomba M, Tamanini M (2000) The bentonites in pelotherapy: chemical, mineralogical and technological properties of materials from Sardinia deposits (Italy). Appl Clay Sci 16:117–124
14. López-Galindo A, Viseras C, Cerezo P (2007) Compositional, technical and safety specifications of clays to be used as pharmaceutical and cosmetic products. Appl Clay Sci 36:51–63
15. Kogel JE, Lewis SA (2001) Baseline studies of the clay minerals society source clays: chemical analysis by inductively coupled plasmamass spectroscopy (ICP-MS). Clays Clay Miner 49(5):387–392
16. Carretero MI, Pozo M (2010) Clay and non-clay minerals in the pharmaceutical and cosmetic industries Part II. Active ingredients. Appl Clay Sci 47(3–4):171–181
17. Rebelo M, Viseras C, López-Galindo A, Rocha F, Silva EF (2011) Characterization of Portuguese geological materials to be used in medical hydrology. Appl Clay Sci 51:258–266
18. FDA (2013) Guideline for elemental impurities, Q3D. Available at: http://www.fda.gov/downloads/drugs/guidancecompliancer egulatoryinformation/guidances/ucm371025.pdf. Accessed May 2015.
19. IAEA (2003) Extent of environmental contamination by naturally occurring radioactive material (norm) and technological options for mitigation. Technical Reports Series No. 419. International Atomic Energy Agency, Vienna
20. UNSCEAR (2010) Sources and effects of ionizing radiation. Volume I: Sources. Report to the General Assembly Scientific Annexes A and B. UNSCEAR 2008 Report. United Nations Scientific Committee on the Effects of Atomic Radiation. United Nations sales publication E.10.XI.3. United Nations, New York
21. Maxwell O, Wagiran H, Ibrahim N, Lee SK, Embong Z, Ugwuoke PE (2015) Natural radioactivity and geological influence on subsurface layers at Kubwa and Gosa area of Abuja, Northcentral Nigeria. J Radioannal Nucl Chem. 303(1):821–830
22. Plant JA, Reeder S, Salminen R, Smith DB, Tarvainen T, De Vivo B, Peterson MG (2003) The distribution of uranium over Europe: geological and environmental significance. Appl Earth Sci 256(3):473–480
23. Noce CM, Machado N, Teixeira W (1998) U-Pb geocronology of gneisses and granitoids in the Quadrilátero Ferrífero (southern São Francisco Craton): ages constrains for Archean and Paleoproterozoic magmatism and metamorphism. Revista Brasileira de Geociências 28:95–102
24. Quéméneur JJG, Noce CM (2000) Geochemistry and petrology of felsic and mafic suítes related to the Paleoproterozoic Transamazonian Orogeny in Minas Gerais, Brazil. Revista Brasileira de Geociências. 30:87–90
25. IAEA (1990) TECDOC—564 Practical aspects of operating a neutron analysis laboratory. International Atomic Energy Agency, Vienna
26. Currie LA (2009) Nomenclature in evaluation of analytical methods including detection and quantification capabilities (IUPAC Recommendations 1995). Pure Appl Chem 67(10):1699–1723
27. Cutshall NH, Larsen LH, Olsen CR (1983) Direct analysis of 210Pb in sediment samples: self-absorption corrections. Nucl Instrum Methods Phys Res Sect 206:309–312
28. Rudnick RL, Gao S (2003) Composition of the continental crust. In: Rudnick RL (ed) The crust, vol. 3. Elsevier, Amsterdam, pp 1–64
29. Sposito V (1989) The chemistry of soils. Oxford University Press, New York
30. Shaheen SM, Tsadilas CD, Rinklebe J (2013) A review of the distribution coefficients of trace elements in soils: influence of sorption system, element characteristics, and soil colloidal properties. Adv Colloid Interface Sci 201–202:43–56
31. Rudnick RL, McLennan SM, Taylor SR (1985) Large ion lithophile elements in rocks from high-pressure granulite facies terrains. Geochim Cosmochim Acta 49(7):1645–1655
32. Carvalho C, Anjos RM, Veiga R, Macario K (2011) Application of radiometric analysis in the study of provenance and transport processes of Brazilian coastal sediments. J Environ Radioact 102(2):185–192
33. UNSCEAR (2000) Sources and Effects of Ionizing Radiation. Volume II: Effects. UNSCEAR 2000 Report. United Nations Scientific Committee on the Effects of Atomic Radiation, 2000 Report to the General Assembly, with scientific annexes. United Nations sales publication E.00.IX.4. United Nations, New York
34. Silva PSC, Oliveira SMB, Farias L, Fávaro DIT, Mazzilli BP (2011) Chemical and radiological characterization of clay minerals used in pharmaceutics and cosmetics. Appl Clay Sci 52(1–2):145–149
35. Santisteban JI, Mediavilla R, López-Pamo E, Dabrio CJ, Zapata MBR, García MJG, Castaño S, Martínez-Alfaro PE (2004) Loss on ignition: a qualitative or quantitative method for organic matter and carbonate mineral content in sediments? J Paleolimnol 32:287–299
36. Stauber JL, Florence TM, Gulson BL, Dale LS (1994) Percutaneous absorption of inorganic lead compounds. Sci Total Environ 145:55–70
37. Orgun Y, Altinsoy N, Sahin SY, Gungor Y, Gultekin AH, Karaham G, Karaak Z (2007) Natural and anthropogenic radionuclides in rock sand beach sands from Ezine region (canakkale), Western Anatolia, Turkey. Appl Radiat Isot. 65:739–747
38. Taskin H, Karavus M, Ay P, Topuzoglu A, Hindiroglu S, Karahan G (2009) Radionuclide concentrations in soil and life time

cancer risk due to the gamma radioactivity in Kirklareli, Turkey. J Environ Radioact 100:49–53
39. Ramasamy V, Paramasivam K, Suresh G, Jose MT (2014) Function of minerals in the natural radioactivity level of vaigai river sediments, Tamilnadu, India—Spectroscopical approach. Spectrochim. Acta, Part A: molecular and biomolecular. Spectroscopy 117(3):340–350
40. ICRP—International Commission on Radiological Protection (1991) ICRP Publication No. 60. Pergamon
41. ICRP—International Commission on Radiological Protection (1996) Conversion coefficients for use in radiological protection against external radiation ICRP Publication No 74. Pergamon, Oxford
42. Durham JS (2006) VARSKIN 3: A Computer Code for Assessing Skin Dose from Skin Contamination. NUREG/CR-6918. U.S. Nuclear Regulatory Commission, Washington, DC
43. ICRP—International Commission on Radiological Protection (2007) The 2007 Recommendations of the International Commission on Radiological Protection, ICRP publication, p 103